Environmental Research 298 (2026) 124292

Contents lists available at ScienceDirect

Environmental Research

journal homepage: www.elsevier.com/locate/envres

Radiofrequency exposure to LTE signal does not alter cancer-related endpoints in human neuroblastoma cell model either alone, or co-exposed to menadione or Wi-Fi signal

Mariateresa Allocca, Maria Rosaria Scarfì, Stefania Romeo, Anna Sannino, Valentina Peluso, Olga Zeni *

National Research Council of Italy (CNR) – Institute for Electromagnetic Sensing of the Environment (IREA), Via Diocleziano 328, 80124, Naples, Italy

ARTICLE INFO

Keywords:
4G-LTE signal
Cancer-related endpoints
Combined exposure
Human neuroblastoma cells
In vitro
Menadione
Wi-Fi

ABSTRACT

Despite the long-term evolution (LTE) signal, also known as fourth generation (4G) technology, is the most employed and widely deployed system for telecommunications, only a few *in vitro* studies are devoted to assessing the biological effects related to exposure to LTE alone and in combination with other agents. To the best of our knowledge, the effect of simultaneous exposure to 4G LTE with other frequencies/signals has not been evaluated in any of these studies.

In the present study we investigated the non-thermal carcinogenic effect of LTE signal under a co-exposure realistic scenario. Human neuroblastoma cells (SH-SY5Y) were exposed for 3 h to 1950 MHz LTE signal, either alone or in combination with the chemical agent menadione. Moreover, the effect of simultaneous exposure to 1950 MHz, 4G LTE signal and 2450 MHz Wireless-Fidelity (Wi-Fi) signal was also evaluated to account for possible effects due to the co-existence of these frequencies/signals. A waveguide-based exposure system, well characterized from dosimetric and experimental point of view, was used, and two specific absorption rate values, 0.3 and 1.25 W/kg, were tested in all cases. Cancer-related endpoints such as reactive oxygen species formation, apoptosis, and cell cycle progression were assessed in flow cytometry assays. In our experimental conditions, neither LTE exposure alone nor LTE and menadione co-exposure or multiple LTE and Wi-Fi exposure influenced the investigated cellular parameters in SH-SY5Y cells.

1. Introduction

Alongside the technological revolution, the last two decades have witnessed a massive diffusion of multi-source electromagnetic fields (EMF) operating at different frequencies, with a trend that will definitely continue (Mattsson et al., 2018), thus exhacerbating the longstandig debate on possible health effects under non-thermal exposure regimen. As a matter of fact, the only established effect of RF-EMF is the increase of temperature due to the absorption of electromagnetic energy by the body tissues, but effects have been reported in the literature also under non-thermal exposure regimen with controversial results (ICNIRP, 2020, 2025).

As a result of the recent advances in wireless communication, the human population is currently exposed to radiofrequency (RF) EMF emitted by multiple sources and related to different technology standards, with the prevalence of fourth (4G) and fifth (5G) generation signals (Betta et al., 2022; Bonato et al., 2022; Chiaraviglio et al., 2024; Miclaus et al., 2023). These signals add to Wi-Fi, short for Wireless Fidelity, commonly used to connect devices and for internet access, that can be found in private homes, schools, workplaces, in cities and public transport.

It is evident that the co-existence of several technologies, operating at different frequencies and signals, contributes to human exposure to EMF and raises the question of the possible effects that could be associated with the exposure to RF from multiple sources. This aspect has also been recently highlighted by the International Commission on Non-Ionizing Radiation Protection (ICNIRP) (ICNIRP, 2025) and it is the focus of the EU Commission in the framework of the Horizon Europe research and innovation programme.

In such a complex scenario, particularly with the deployment of 5G

* Corresponding author. CNR- Institute for Electromagnetic Sensing of the Environment (IREA), Via Diocleziano 328, 80124, Naples, Italy.
E-mail addresses: allocca.m@irea.cnr.it (M. Allocca), scarfi.mr@irea.cnr.it (M.R. Scarfì), romeo.s@irea.cnr.it (S. Romeo), peluso.v@irea.cnr.it (V. Peluso), zeni.o@irea.cnr.it (O. Zeni).

https://doi.org/10.1016/j.envres.2026.124292
Received 30 October 2025; Received in revised form 23 February 2026; Accepted 14 March 2026
Available online 16 March 2026
0013-9351/© 2026 The Authors. Published by Elsevier Inc. This is an open access article under the CC BY license (http://creativecommons.org/licenses/by/4.0/).

network, attention has been devoted to developing innovative approaches to characterize RF-EMF exposure induced under various usage scenarios and by multiple sources (Liu et al., 2024; Veludo et al., 2025). Such information is crucial for health risk assessment and for the definition of adequate exposure standards (ICNIRP, 2020; Schilling et al., 2021).

The same attention has not been paid in the case of the experimental studies which mainly address the biological effects of RF exposure at single frequencies or signals of different characteristics, while considering mostly chemical treatments as a possible agent for co-exposure to mimic the real-life human exposure to EMF and other environmental agents. Herein, co-exposures are defined as multiple when different RF frequencies/signals are applied, and as combined in the case of exposure to RF and other physical or chemical agents. According to Kostoff and Lau (2013), such responses can be classified as: a) additive effect: the effect of two agents is the sum of the effects of each of them independently applied; b) antagonistic/protective effect: the effect is lower than the sum of the contribution of the single treatments; c) potentiative effect: the increased effect of an agent by concurrent action of another agent that does not have a stand-alone effect; d) synergistic effect: the effect of two or more agents is significantly greater than the sum of the effects of each agent administered alone.

With respect to the study of combined exposures, several electromagnetic conditions, mainly related to frequencies and signals of 2G and 3G mobile phone technology, have been considered in the literature and several protocols for the administration of the agent for co-exposure (before, concurrent or after RF exposure) have been applied, with results strictly depending on the biological model, the administration protocol of the agent for co-exposure and on the RF exposure parameters (SCENIHR, 2015; SSM, 2024). For many years, our research group has been involved in the study of the combined exposure of mammalian cells to RF and other physical or chemical agents. We demonstrated that RF exposure, with several frequencies, signals (2G, 3G and 4G technologies), and Specific Absorption Rate (SAR) values in almost all cases did not induce biological effects when administered alone. Conversely, RF pre-exposure of several cell models resulted effective in providing protection against the damaging effects of subsequent chemical or physical treatments, with the effect strictly depending on the experimental conditions adopted, both biological and electromagnetic (Falone et al., 2018; Romeo et al., 2020; Sannino et al., 2009, 2011, 2014, 2019, 2022, 2024a, 2024b, 2025; Zeni et al., 2012, 2021). Similar findings were also reported by other independent research groups in different cell types (Cao and Tong, 2014; Gapeyev and Lukyanova, 2015; He et al., 2016, 2017; Ji et al., 2016; Mortazavi et al., 2017; Zong et al., 2015).

A few experimental (*in vivo* and *in vitro)* studies address the effects of multiple frequencies/signals exposure, that are mainly carried out by a Korean research group. In these studies, only frequencies/signals used by 2G and 3G technologies have been considered with negative results (Hong et al., 2012; Jin et al., 2011, 2013; Kang et al., 2014; Kim et al., 2012; Lee et al., 2009, 2011a, 2011b, 2012, 2016). In addition, negative results were also recorded in two investigations carried out by independent research groups (López-Furelos et al., 2012; Shirai et al., 2017). Also, there are few studies investigating the biological and health effects of Wi-Fi signal exposure, that suggest lack of detrimental health effects from exposure below regulatory limits, as reviewed by Dongus and co-workers (Dongus et al., 2022). Moreover, none of them used Wi-Fi in combination with other frequencies/signals in use for mobile communications. If the health effects of Wi-Fi exposure are considered unlikely, because Wi-Fi devices and access points are low powered (typically 0.1 Watt), the effects due to interaction with other RF signals cannot be *a priori* excluded and are worthy of investigation.

Building on the current RF exposure scenario and on the existing experimental studies, the current *in vitro* study focused on the 1950 MHz 4G LTE signal, which is still the most used for mobile communication worldwide, to address possible combined effect with menadione (MD), on one side, and the effect of multiple exposure with Wi-Fi signal (2450 MHz), on the other side. MD is a semiquinone largely used in the studies dealing with oxidative stress. It is a well-known reactive oxygen species (ROS) inducer (Loor et al., 2010). In addition, MD has been also reported to induce apoptosis (Oztopcu-Vatan et al., 2015; Sa et al., 2009).

We used here a human neuroblastoma cell model, which in our previous studies resulted responsive to combined exposures under different EM conditions. An exposure apparatus, employing waveguide applicators, was previously characterized in our laboratory and used to expose cell cultures to 0.3 W/kg and 1.25 W/kg SAR levels. ROS formation, apoptosis and cell cycle progression were analyzed to investigate possible alteration of cell physiology due to 4G LTE exposure alone, in combination with MD at two concentrations or with Wi-Fi signal.

2. Material and methods

2.1. Reagents

Dulbecco's modified Eagle's medium (DMEM), foetal bovine serum (FBS), phosphate buffer saline (PBS) and Trypsin-EDTA were from Microgem (Napoli, Italy). GlutaMAX was from Gibco™ by Thermo Fisher Scientific Inc. (Waltham, MA, USA). Penicillin/streptomycin solution was from HiMedia (Mumbai, India). Menadione (MD), 2′,7′-Dichlorodihydrofluorescein diacetate (DCFH-DA), propidium iodide (PI), Triton X-100 and Mitomycin-C (MMC) were from SIGMA (St. Louis, MO, USA). Sodium citrate dihydrate was from J. T. Baker (Deventer, The Netherlands). Trypan blue staining solution was from Logos Biosystems (Anyang-City, South Korea). Apoptosis Detection kit was from Leinco Technologies (Fenton, MO, USA).

2.2. Radiofrequency EMF exposure setup and dosimetry

A waveguide-based exposure system was used to expose cell cultures to 1950 MHz, LTE signal, that was detailed and sketched in (Sannino et al., 2024b). The same setup was optimized here to carry out simultaneous exposure of cell cultures to 1950 MHz, LTE and 2450 MHz, Wi-Fi signals. In both cases, cell cultures were exposed to 0.3 or 1.25 W/kg SAR under well characterized environmental and electromagnetic conditions.

2.2.1. Single frequency/signal scenario

The LTE signal, generated through a code built inhouse in Matlab (2019) (MathWorks, Natick, MA, USA), was supplied by the E4432B ESG-D RF generator (Agilent, Santa Clara, CA, USA) to the microwave amplifier (AM38A-0925-40-43, MALTD, Bristol, England). Then the signal was split by the −6 dB power splitter (HP11667A −6 dB, Hewlett-Packard, Santa Clara, CA, USA) into two output signals which were sent to two bidirectional power sensors (The NRT-Z43 bidirectional, Rohde & Schwarz, Munich, Germany) to feed two short-circuited WR430 waveguides (350 mm long) (SAIREM, Neyron, France). Two coaxial-to-waveguide adapters (R213A2; VSWR: 1.05; Maury Microwave, Ontario, CA, USA) allowed the connection to the feeding sides. The waveguides were placed inside a cell culture incubator (Forma Scientific, Freehold, NJ, USA) together with a third one, used for sham-exposure. Numerical and experimental dosimetry was previously carried out and reported in (Romeo et al., 2013). The exposure parameters setting and remote control of the generator and power sensors occurred via a Labview programme (National Instruments, Austin, TX, USA).

2.2.2. Multiple frequency/signal scenario

The setup for multiple exposures is shown in Fig. 1. The LTE signal, generated as described above, and the Wi-Fi signal, generated by a SMM100A RF generator (Rohde&Schwarz, Munich, Germany) with IEEE 802.11 option enabled, with a relative contributions to the total SAR of approximately 48% for 1950 MHz and 52% for 2450 MHz. The two signals were sent to the power combiner (PD2020, InNSTOCK wireless components, NJ, USA) and the output signal was amplified and

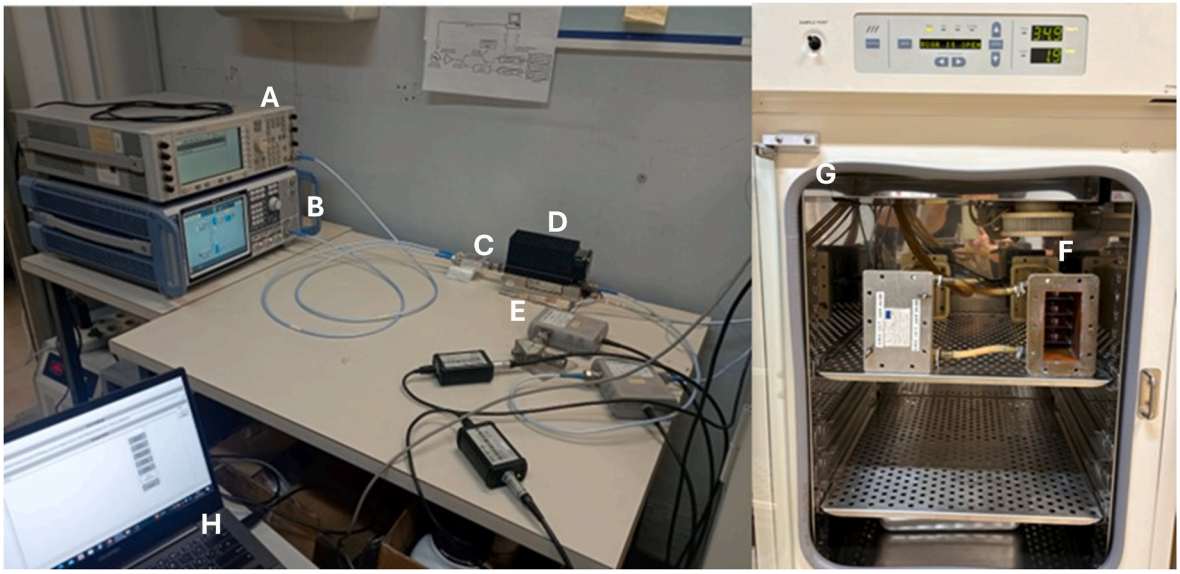


Fig. 1. Configuration and components of the setup employed for simultaneous exposures of four samples to 1950 MHz (LTE signal) and 2450 MHz (Wi-Fi) RF-EMF. A and B: RF generators; C: power combiner; D: microwave amplifier; E: bidirectional power sensor; F: waveguide; G: cell culture incubator; H: PC for remote control.

sent to one short-circuited waveguide by means of the power sensor. Two waveguides, one for RF and one for sham-exposure, were placed inside a standard cell culture incubator. The Virtual NRT software (Rohde & Schwarz, Munich, Germany) was used to remotely control the power sensor, and the levels of incident and reflected power were recorded throughout the exposure to verify the stability of SAR levels.

Dosimetry was performed to get high efficiency and uniformity of SAR distribution in four samples to be simultaneously exposed to 1950 MHz and 2450 MHz. Customized 30 mm diameter Pyrex dishes were used for cell cultures, which allowed to reduce the non-uniformity degree to acceptable level in the case of 2450 MHz (Romeo et al., 2013).

For numerical dosimetry, carried out by CST Microwave Studio 2024 platform (Dassault Systèmes Simulia, Paris, France), parametric simulations were run to identify the distance of the samples' center to the short-circuit that maximizes the efficiency and uniformity of SAR distribution in the four samples at both frequencies. The average SAR over the sample per unit of incident power (W/kg/W), was calculated as an indicator of the average specific efficiency. The Coefficient of Variation (CV), defined as the standard deviation of the SAR over the mean value, was adopted as an indicator of the SAR non-uniformity degree. Since the SH-SY5Y cell model grows adherent to the bottom of the dish, both parameters were calculated for the Whole Sample (WS) and for the Bottom Layer (BL). The overall efficiency (absorbed to incident power ratio) was also calculated.

The rectangular waveguide (inner transversal dimensions: 109.2 mm × 54.6 mm) was modelled as perfectly conductive with the longitudinal axis and narrow side horizontal, to achieve the condition of E vector parallel to the sample layer (Fig. 2, Panel A). The four samples were modelled as DMEM cylinders (27.2 mm diameter, 3 mm thickness) placed inside four 30 mm, Pyrex dishes and located on a four-layer Plexiglas stand (Fig. 2, Panel B). Electromagnetic properties of materials are reported in Table 1, while the mass density of DMEM samples was set at 1060 kg/m^3, according to data reported in the literature (Calabrese et al., 2006).

From the simulations, the distance between the samples' centers and the short circuit that maximizes efficiency and uniformity of SAR,

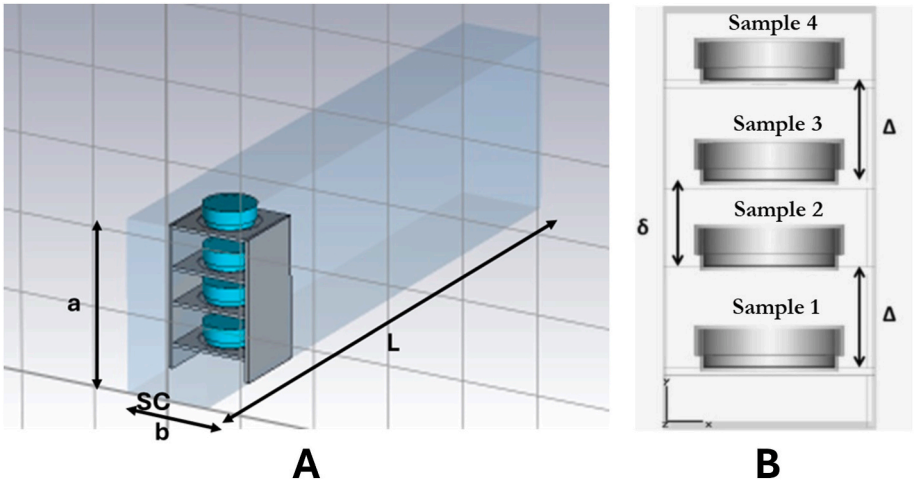


Fig. 2. Panel A: Geometric model of the waveguide (a = 109.2 mm; b = 54.6 mm; L = 350 mm) and of the four samples in 30 mm Pyrex dishes on the Plexiglas stand. SC: Short Circuit at 73.6 mm from the samples' centers. Panel B: detailed sketch of the four samples on the Plexiglas stand. The relative distances between the samples (δ = 22 mm; Δ = 26 mm) are set in such a way to obtain a 1:4 SAR ratio between the distal (sample 1 and sample 4) and the central (sample 2 and sample 3) positions of the stand.

Table 1
Electromagnetic properties of materials set for numerical simulations.

	Pyrex		Plexiglass		DMEM	
	ε_r	σ [S/m]	ε_r	σ [S/m]	ε_r	σ [S/m]
1950 MHz	4.7	0	2.6	0	70	2.45
2450 MHz	4.7	0	2.6	0	70	2.9

resulted to be 73.6 mm. Table 2 shows the average SAR at 1 W incident power and CV, for each sample (both whole sample and bottom layer) at 1950 and 2450 MHz. The CV is around the desired value of 0.3 at 1950 MHz, and slightly higher (0.34-0.36), but still acceptable, at 2450 MHz (Romeo et al., 2013). Fig. 3 presents the SAR distribution in the bottom layer, and the histograms of the SAR normalized to the average value for each sample exposed to 1950 and 2450 MHz.

Measurements were performed to calculate the absorbed power (difference between incident and reflected powers, neglecting the waveguide power losses), and consequently to derive the average SAR levels (as absorbed power divided by the mass) to be compared to the ones gained by numerical simulations. The measured average SAR in the central (SAR_c) and in distal (SAR_d) samples and the overall efficiency were in satisfying agreement with the results of numerical simulations, as reported in Table 3.

To verify the average levels and stability of SAR and to exclude heating of the sample under the selected exposure conditions, power and temperature measurements were performed by exposing samples for 3 h at 1.25 W/kg average SAR in the central positions and 0.3 W/kg average SAR in the distal positions. The temperature measurements were performed by using a UMI4 thermometer with a fiber optic probe (FISO Technologies, Quebec, Canada) inserted in one of the samples exposed to 1.25 W/kg SAR. Fig. 4A presents the average SAR over 3-h exposure time, in the central samples, as obtained by measurement of the incident and reflected powers. Fig. 4B presents the results of temperature measurements (fiber optic inserted in one of the central samples) over 3-h exposure-time. Temperature measurements were performed starting 1 h before and ending 1 h after RF exposure to ensure temperature equilibration and exclude any RF-induced heating.

2.3. Cell culture maintenance and experimental procedures

Human SH-SY5Y Neuroblastoma Cell Line (ATCC, Cat. No. CRL2266, Rockville, MD, USA) was cultured in 4.5 g/L glucose DMEM, supplemented with 10% heat-inactivated FBS, 2 mM Glutamax, 100 U/mL penicillin, and 0.1 mg/mL streptomycin. Cell cultures, periodically checked for mycoplasma infection, were maintained under standard conditions in an incubator at 37 °C and 5% CO_2 humidified atmosphere. Fresh culture medium was supplied every 48 h and cells were split once a week by 200 mg/ml trypsin treatment. For the sake of consistency and reproducibility of the experiments, the same batch of reagents was used, and cells from passage 3 to 10 were employed.

2.3.1. Exposure to 1950 MHz, LTE signal alone and combined with menadione

1×10^6 cells were seeded in 35 mm cell culture dishes (Corning Inc., Corning, NY, USA) and grown for 72 h in 3 ml complete medium. Cells were exposed for 3 h (from 48 to 51 h after seeding) at 1950 MHz, LTE signal (0.3 or 1.25 W/kg SAR). For each independent experiment, eight randomly assigned cultures were set up: negative control (incubator), sham-exposed (Sh), RF-exposed at 0.3 W/kg (0.3 W/kg) and RF-exposed at 1.25 W/kg (1.25 W/kg), MD-treated (MD), sham-exposed and MD treated (Sh + MD), RF-exposed at 0.3 W/kg and MD treated (0.3 W/kg + MD), RF-exposed at 1.25 W/kg and MD treated (1.25 W/kg + MD). MD concentration and treatment duration were selected downstream of dose-response curves set up in preliminary experiments and reported in Supplementary Figs. S1 and S2 for ROS detection and apoptosis, respectively. In particular, 5 μM and 20 μM concentrations were selected in both cases and given for 10 min and 30 min at the end of RF exposure for ROS and apoptosis, respectively.

2.3.2. Multiple exposure to LTE and Wi-Fi signals

8.5×10^5 cells were seeded in customized 30 mm Pyrex dishes and grown for 72 h in 1.75 ml of complete medium. The suitability of customized dishes to host cell cultures was verified by setting up 4 days growth curves in Pyrex dishes by using standard Polystyrene dishes as reference control. Cell growth was assessed by means of Trypan Blue Dye Exclusion (TBDE) test and the results are presented in Supplementary Fig. S3.

Cells were simultaneously exposed for 3 h (48-51 h) at 1950 MHz, LTE signal and 2450 MHz, Wi-Fi signal (0.3 or 1.25 W/kg SAR). For each independent experiment, four randomly assigned cultures were set up: negative control (incubator), sham-exposed (Sh), RF-exposed at 0.3 W/kg (0.3 W/kg) and RF-exposed at 1.25 W/kg (1.25 W/kg).

For both combined and for multiple exposures, at least three independent experiments were carried out blinded: samples were coded in such a way that the operator performing the analysis was not aware of the treatment. The code was broken only after completion of the analysis.

2.4. ROS detection

The formation of ROS was assessed by using the probe 2′,7′-Dichlorodihydrofluorescein diacetate (DCFH-DA) (LeBel et al., 1990). At the end of the culture period, the cells were collected by trypsinization and washed twice with cold PBS. DCF fluorescence from 15000 events was acquired by flow cytometry and visualized via CellQuest software (BD Biosciences, NJ, USA). The percentage of DCF positive cells was calculated by using FlowJo software (TreeStar, OR, USA), setting the threshold value on the background DCF fluorescence of the untreated control. Cells treated for 10 min with 20 μM MD served as positive control.

2.5. Apoptosis detection

Apoptosis was assayed by double staining with Annexin V-FITC and propidium iodide (PI) in accordance with the instruction of the apoptosis detection kit manufacturer's. At the end of the culture period, the cells were collected by trypsinization and counted by TBDE assay. 3×10^5 cells were washed twice with cold PBS and incubated for 10 min at room temperature in the dark with Annexin V-FITC and PI. Data from 15000 events were acquired by flow cytometry via CellQuest software and analyzed by using FlowJo software. Cells were distributed in different quadrants of the dot plot: early apoptotic cells at the bottom

Table 2
Average SAR at 1 W incident power and coefficient of variation (CV) for each sample (Whole Sample, WL, and Bottom Layer, BL) at 1950 and 2450 MHz.

Frequency [MHz]	Sample	Average SAR [W/kg/W]				Coefficient of variation (CV)			
		1	2	3	4	1	2	3	4
1950	**WS**	28.4	112.6	113.4	28.3	0.31	0.31	0.31	0.31
	BL	24.1	101.5	106.1	27.8	0.33	0.31	0.30	0.29
2450	**WS**	42	153.5	154.1	41.6	0.35	0.36	0.36	0.36
	BL	37.6	136.8	140.1	37.7	0.34	0.34	0.34	0.34

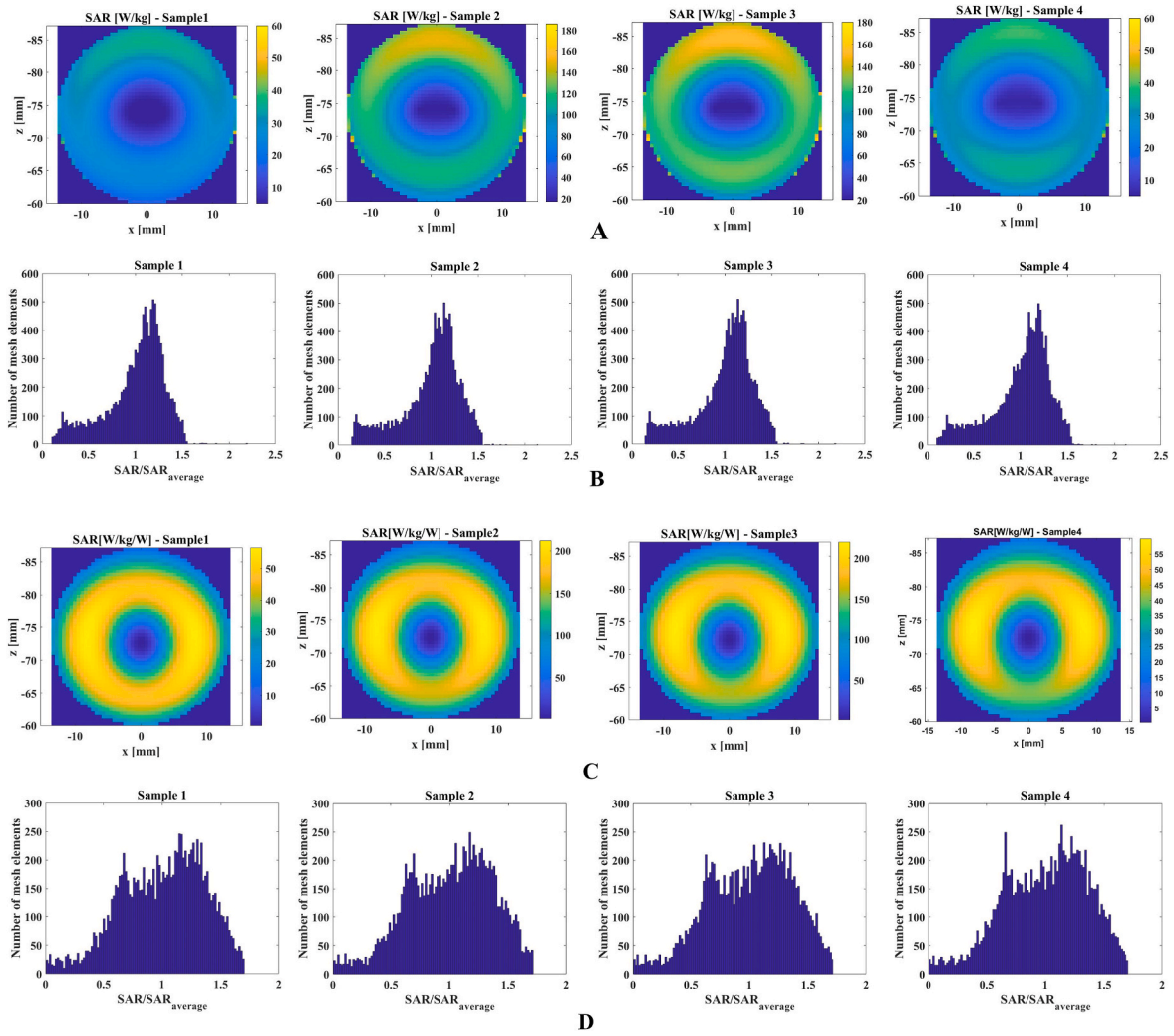


Fig. 3. SAR distribution in the bottom layer of each sample, and histograms of the whole sample SAR normalized to the average value, obtained at 1950 MHz (Panel A and B) and 2450 MHz (Panel C and D).

Table 3
Comparison between average SAR and overall efficiency obtained by simulations and by power measurements. SAR_c and SAR_d are the SAR levels in the samples of central and distal positions of the stand, respectively.

Frequency [MHz]	Simulations			Power measurements		
	SAR_c [W/kg/W]	SAR_d [W/kg/W]	Overall Efficiency	SAR_c [W/kg/W]	SAR_d [W/kg/W]	Overall Efficiency
1950	113.4	28.3	52 %	136.7 ± 3.1	34.2	60 % ± 2%
2450	154.1	41.6	69 %	165.5 ± 0.25	44.7	72% ± 3%

right (Annexin V- $FITC^+/PI^-$), late apoptotic cells at the top right (Annexin V- $FITC^+/PI^+$) and necrotic cells (Annexin V- $FITC^-/PI^+$) at the top left; and the percentage of cells was quantified in each quadrant. Cells treated for 30 min with 20 μM MD served as positive control.

2.6. Cell cycle progression

The cell cycle was assayed by cell membrane permeabilisation and PI staining as previously described (Cotugno et al., 2012). Briefly, at the end of the culture period, the cells were collected by trypsinization and counted by TBDE assay. 5×10^5 cells were washed twice with cold PBS and incubated for 30 min at 4 °C in the dark with 50 μg/ml PI, 33 mM sodium citrate, pH 8, and 0.1% Triton X-100 (1:2 dilution with absolute DMEM). Data from 25000 events were acquired by a flow cytometer via CellQuest software. The percentage of cells in G0/G1, S, and G2/M stages was determined by using FlowJo software. Cells treated for 16 h with 1 μg/ml MMC, a known cytotoxic agent, served as positive control after setting a dose-response curve (Supplementary Fig. S4).

2.7. Statistical analysis

Results are shown as the mean ± standard deviation (SD) of at least three independent experiments. Data were analyzed by two tailed unpaired Student's *t*-test and the differences were considered statistically significant for p values below 0.05 (*$p < 0.05$; **$p < 0.01$; ***$p < 0.001$).

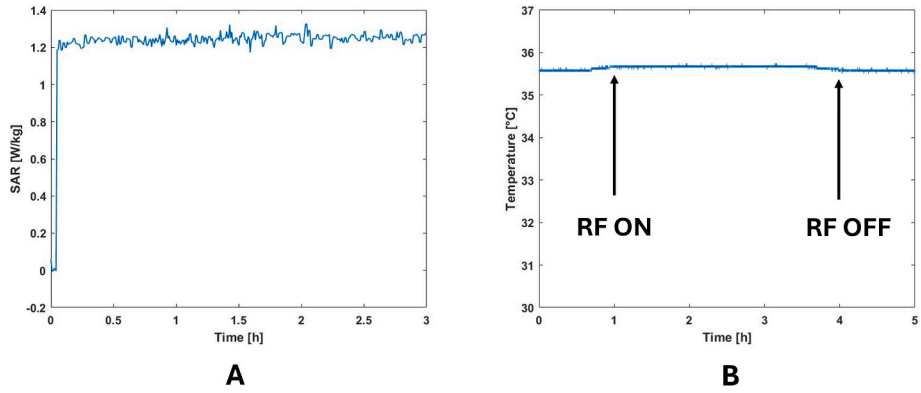


Fig. 4. Average SAR (Panel A) and temperature (Panel B) in sample exposed simultaneously to 1950 and 2450 MHz for 3 h at 1.25 W/kg SAR.

3. Results

3.1. LTE exposure does not impair ROS, apoptosis and cell cycle

The effect of 3-h LTE exposure (0.3 and 1.25 W/kg SAR) is presented in Fig. 5 for ROS formation (Panel A), apoptosis (Panel B) and cell cycle progression (Panel C), whereas in Supplementary Fig. S5, flow cytometry fluorescence histograms (Panel A and Panel C) and dot plots (Panel B) of representative experiments are reported.

RF exposure at both SAR levels did not affect the parameters investigated (Sh *vs*. 0.3 W/kg; Sh *vs*. 1.25 W/kg) whereas a statistically significant increase was detected when positive control samples were compared to incubator controls. The background level of each endpoint was not impaired in sham samples (Sh *vs.* incubator) that served as control in the co-exposure experiments.

3.2. LTE exposure does not modify the MD-induced effect on ROS and apoptosis

To evaluate the combined effect of LTE and MD, cells were exposed for 3 h to two SAR levels (0.3 and 1.25 W/kg) and subsequently treated with two MD concentrations, 5 and 20 μM provided for 10 min and 30 min for ROS and apoptosis, respectively. Fig. 6 presents the results of ROS formation (Panel A) and apoptosis induction (Panel B). In Supplementary Fig. S6, flow cytometry fluorescence histograms and dot plots for ROS (Panel A) and apoptosis (Panel B), respectively of representative experiments are reported. No effect was detected by comparing RF exposed and MD treated samples to the respective sham-exposed and MD treated ones (RF + MD *vs*. Sham + MD), although slight, not statistically significant variations were recorded by comparing samples sham exposed and MD-treated with samples RF exposed and MD-treated.

3.3. RF EMF exposure administered under multiple frequency/signal scenario does not impair ROS, apoptosis and cell cycle

The results of 3-h multiple exposure to 1950 MHz LTE and 2450 MHz Wi-FI at SAR levels of 0.3 and 1.25 W/kg are presented in Fig. 7 in terms of ROS formation (Panel A), apoptosis (Panel B) and cell cycle progression (Panel C). In all cases no effect was detected by comparing sham exposed samples *vs*. RF exposed ones. Samples treated with 20 μM MD for ROS and apoptosis and with 1 μg/ml of MMC for cell cycle served as positive controls and induced a statistical significant increase in the analyzed endpoints, as expected.

4. Discussion

Humans are currently exposed to a complex mixture of EMFs of several frequencies/signals with specific characteristics and to chemical compounds of different doses as a result of recently introduced technologies. Recently, the 5G network has been introduced but the 4G LTE signal remains prevalent, contributing largely to the above-mentioned scenario. Despite that, a few experimental studies covering cancer-related endpoints after 4G LTE exposure/co-exposure have been carried out, as discussed in Sannino et al. (2024b). In addition, two more recent papers report on the impact of LTE RF-EMF on thyroid hormones in young mice exposed to 4 W/kg SAR for 8 h daily over 4 weeks (Kim et al., 2024) and on hematological and reproductive systems, liver, and kidney of Wistar rats exposed for 2 h/day for 56 days to 0.0062 W/kg (Gautam et al., 2024). On the whole, the results available are conflicting.

In the current study, we analyzed cancer-related endpoints in SH-SY5Y cells after 3-h exposure to 4G LTE given alone, in combination with MD at two concentrations, or with Wi-Fi. In all cases, two SAR values were tested (0.3 and 1.25 W/kg).

MD was selected as chemical for combined exposures since in previous studies we demonstrated that pre-exposures of SH-SY5Y to RF at different frequencies and modulation schemes are able to reduce the MD-induced damage by enhancing antioxidant scavenging efficiency and autophagy and restoring DNA repair efficiency (Falone et al., 2018; Sannino et al., 2022, 2024a).

It has been shown that the contribution of Wi-Fi to total RF-EMF exposure is relatively low, typically below 10% (Gallastegi et al., 2018; Jalilian et al., 2019) and the literature does not suggest health effects from Wi-Fi exposure (Dongus et al., 2022). For this reason, studying the effects of Wi-Fi together with other RF signals is even more interesting than studying the effects of Wi-Fi exposure alone.

With reference to real life co-exposure scenario, mostly chemicals were considered as agents for combined exposures, and only a few investigations address RF exposure to multiple frequencies/signals. In the former case, the outcome varies on the basis of cell type, electromagnetic conditions, and concentration and timing of the agents used, triggering adverse or beneficial effects (Kostoff and Lau, 2013; Verschaeve, 2012). In the latter case, mainly negative results have been reported. In particular, several cell models have been employed to investigate multiple exposure to 837 MHz CDMA and 1950 MHz WCDMA at SAR levels of 4 W/kg (2 W/kg for each signal). The exposure duration varied from a minimum of 1 h to a maximum of 2 h/day for three days, and no alteration in DNA synthesis, cell cycle regulatory proteins in MCF7 cells was found (Lee et al., 2011b). No effect was also recorded on MCF10A in terms of oxidative stress (Hong et al., 2012) and expression of heat shock proteins and mitogen-activated protein kinases (MAPKs) (Kim et al., 2012). Lack of effect was also reported in several neuronal cell models (U87, PC12 or SH-SY5Y) when ROS formation was measured at different time points post-exposure (Kang et al., 2014), and in HT22 hippocampal neurons in terms of cell viability, and proliferation and ROS production. In this study, the authors also found that the Aβ-induced decreased cell proliferation, increased ROS production, or cell death were not modified by the exposure (Lee et al., 2012).

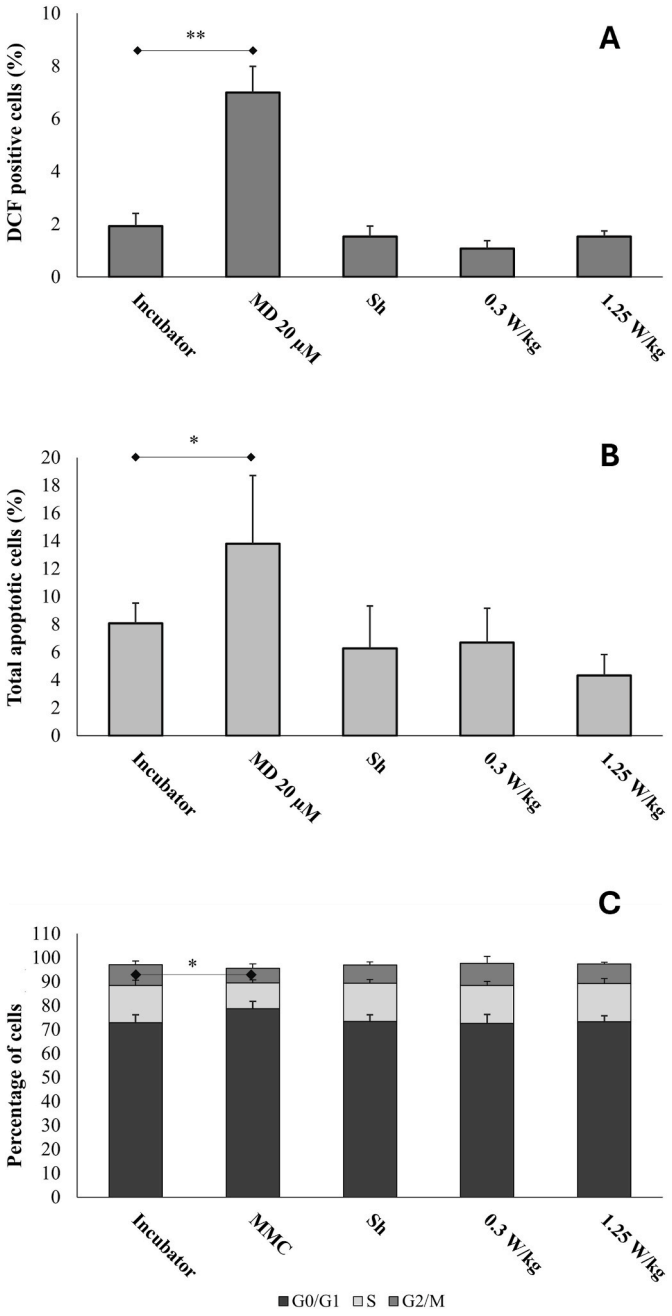


Fig. 5. Effects of 3-h exposure to 1950 MHz, LTE signal (0.3 and 1.25 W/kg). Panel A: ROS formation expressed as percentage of DCF positive cells (mean ± SD of three independent experiments). Treatments with 20 μM MD for 10 min served as positive control. Panel B: percentage of total apoptotic cells (mean ± SD of five independent experiments). Treatments with 20 μM MD for 30 min treatment served as positive control. Panel C: percentage of cells in the different stage of cell cycle (mean ± SD of three independent experiments). Treatments with 1 μg/ml MMC for 16 h served as positive control. Two-tailed unpaired Student's *t*-test: *p < 0.05; **p < 0.01.

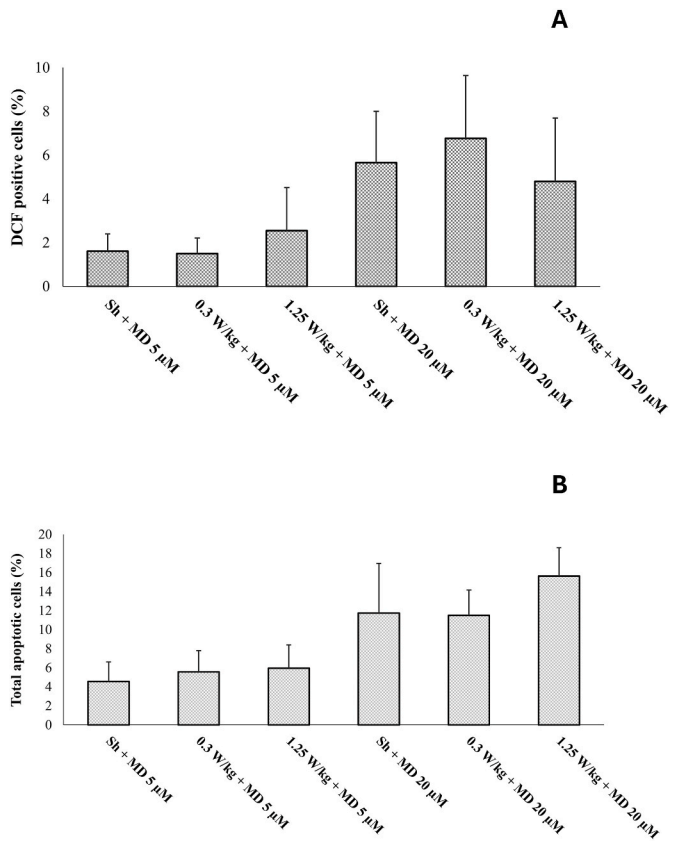


Fig. 6. Effects of 3-h co-exposure to 1950 MHz, LTE signal (0.3 and 1.25 W/kg) and MD (5 and 20 μM). Panel A: ROS formation expressed as percentage of DCF positive cells (mean ± SD of three independent experiments); MD treatments lasted 10 min. Panel B: percentage of total apoptotic cells (mean ± SD of five independent experiments); MD treatment lasted 30 min.

Most of the *in vivo* investigations have been carried out on several rat models under the same multiple exposure conditions employed for *in vitro* studies. No observable effects were found on fetuses of pregnant ICR mice (Lee et al., 2009), on the rat reproductive system of male Sprague-Dawley (SD) (Lee et al., 2012), on immuno-functions of male SD rats (Jin et al., 2012), on several parameters of lymphoma development in AKR-mice, and on several parameters of the endocrine system of SD rats (Jin et al., 2013). Chronic illness and total tumor incidence also resulted unaffected in SD rats although a slightly altered parameters in the blood count and serum chemistry were recorded (Jin et al., 2011). Lopez-Furelos and co-workers investigated the effect of multiple exposure to 900 MHz and 2450 MHz (2 W/kg in total) in male SD rats exposed for 1 h with no effect on cell morphology and apoptosis (López-Furelos et al., 2012). Shirai and coworkers exposed pregnant SD rats to eight different RF signals at frequencies between 800 MHz and 5.2 GHz at SARs of 0.08 and 0.4 W/kg. The results did not show any adverse effects on pregnancy and on the development of rats (Shirai et al., 2017).

In conclusion, with reference to the results here presented and discussed we want to highlight that neither 4G LTE exposure alone nor in combination with MD or Wi-Fi signals does influence ROS formation, apoptosis and cell cycle progression in SH-SY5Y cells in all the conditions tested. These findings also confirm that, under well controlled electromagnetic and biological conditions, LTE exposure alone does not induce cytotoxic effects, in accordance with our previous results, and that the onset of cooperative effect, when present, strictly depends on the experimental conditions adopted (Sannino et al., 2024b). In addition, the results of exposure to LTE and Wi-Fi extend to more recent technologies the absence of effects of simultaneous exposure to two different frequencies/signals.

We want to highlight that this study could be relevant for health risk assessment since it complies with the requirements for a good quality *in vitro* investigation, an issue still critical in bioelectromagnetic research (Paffi et al., 2010; Simko et al., 2016, 2025; Zeni and Scarfì, 2012). At the same time, we recognize that further investigations employing different experimental conditions (cell model, exposure duration, SAR level, chemical treatment and schedule) are required to gain more

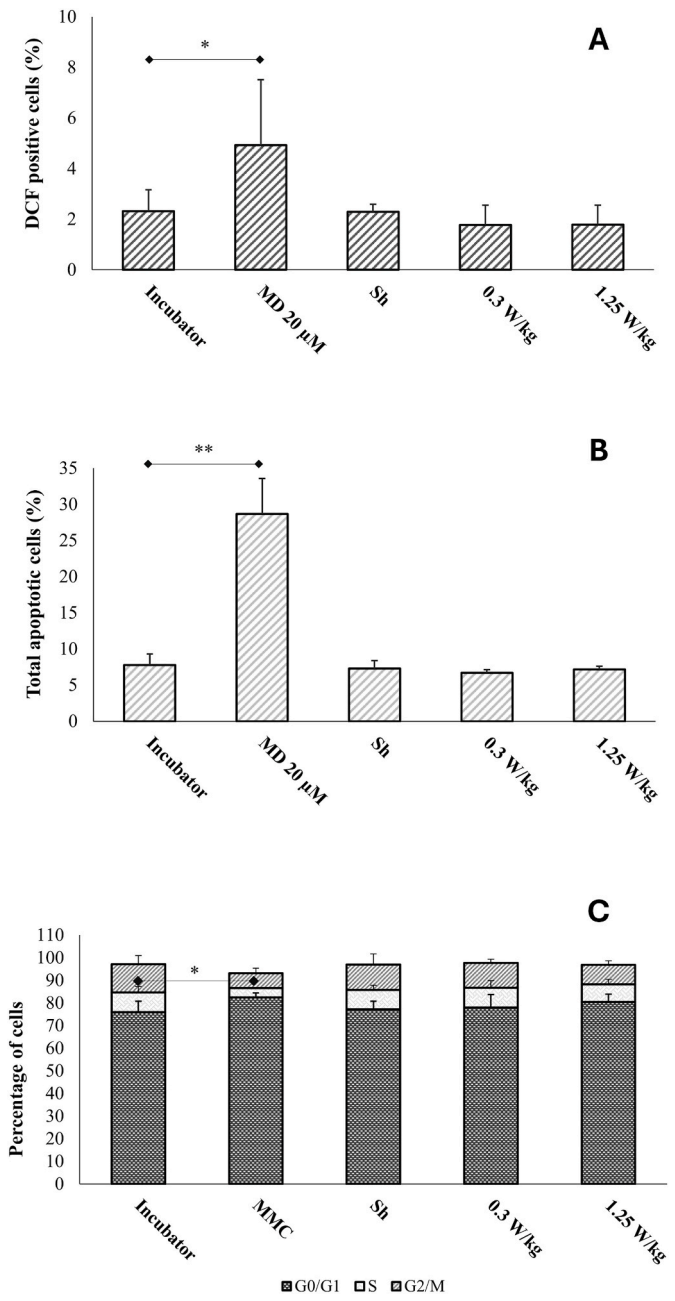


Fig. 7. Effects of 3-h multiple exposure to 1950 MHz, LTE signal and 2450 MHz Wi-Fi signal (0.3 and 1.25 W/kg). Panel A: ROS formation expressed as percentage of DCF positive cells (mean ± SD of six independent experiments); MD: 20 μM for 10 min. Panel B: percentage of total apoptotic cells (mean ± SD of three independent experiments); MD 20 μM for 30 min. Panel C: cell cycle progression (mean ± SD of three independent experiments); MMC 1 μg/ml for 16 h. Two-tailed unpaired Student's *t*-test: *$p < 0.05$; **$p < 0.01$.

information on RF co-exposures.

CRediT authorship contribution statement

Mariateresa Allocca: Writing – review & editing, Writing – original draft, Methodology, Investigation, Formal analysis. **Maria Rosaria Scarfi:** Writing – review & editing, Writing – original draft, Data curation, Conceptualization. **Stefania Romeo:** Writing – review & editing, Writing – original draft, Methodology, Investigation, Formal analysis. **Anna Sannino:** Writing – review & editing, Writing – original draft, Investigation, Formal analysis, Conceptualization. **Valentina Peluso:** Writing – review & editing, Writing – original draft, Methodology, Investigation. **Olga Zeni:** Writing – review & editing, Writing – original draft, Funding acquisition, Data curation, Conceptualization.

Funding sources

This work is part of the European Union's Horizon Europe research and innovation program under grant agreement No. 101057527 (NextGEM) funded by the European Union. Views and opinions expressed are however those of the authors only and do not necessarily reflect those of the European Union. Neither the European Union nor the granting authority can be held responsible for them.

Declaration of competing interest

I declare the absence of competing financial interests or personal relationships that could have appeared to influence the work reported in this paper.

Acknowledgements

The authors gratefully acknowledge Fulvio Schettino (University of Cassino and Southern Lazio, Italy) for fruitful discussion on dosimetry.

Appendix A. Supplementary data

Supplementary data to this article can be found online at https://doi.org/10.1016/j.envres.2026.124292.

Data availability

Data will be made available on request.

References

Betta, G., et al., 2022. Measurements of Human Exposure to EMF from 4G Systems: Some Experimental Issues in Urban Environments. International Conference on Electromagnetic Fields, Signals and Biomedical Engineering, vol.1254. IOP Publishing Ltd Sibiu, Romania.
Bonato, M., et al., 2022. Assessment of human exposure levels due to Mobile phone antennas in 5G networks. Int. J. Environ. Res. Publ. Health 19.
Calabrese, M.L., et al., 2006. A high-efficiency waveguide applicator for in vitro exposure of mammalian cells at 1.95 GHz. IEEE Trans. Microw. Theor. Tech. 54, 2256–2264.
Cao, Y., Tong, J., 2014. Adaptive response in animals exposed to non-ionizing radiofrequency fields: some underlying mechanisms. Int. J. Environ. Res. Publ. Health 11, 4441–4448.
Chiaraviglio, L., et al., 2024. Dominance of smartphone exposure in 5G Mobile networks. IEEE Trans. Mobile Comput. 23, 2284–2302.
Cotugno, R., et al., 2012. Effect of sesquiterpene lactone coronopilin on leukaemia cell population growth, cell type-specific induction of apoptosis and mitotic catastrophe. Cell Prolif. 45, 53–65.
Dongus, S., et al., 2022. Health effects of Wi-Fi radiation: a review based on systematic quality evaluation. Crit. Rev. Environ. Sci. Technol. 52, 3547–3566.
Falone, S., et al., 2018. Protective effect of 1950 MHz electromagnetic field in human neuroblastoma cells challenged with menadione. Sci. Rep. 8, 13234.
Gallastegi, M., et al., 2018. Children's exposure assessment of radiofrequency fields: comparison between spot and personal measurements. Environ. Int. 118, 60–69.
Gapeyev, A.B., Lukyanova, N.A., 2015. Pulse-modulated extremely high-frequency electromagnetic radiation protects cellular DNA from the damaging effects of physical and chemical factors in vitro. Biophysics 60, 732–738.
Gautam, R., et al., 2024. Effects of 4G mobile phone radiation exposure on reproductive, hepatic, renal, and hematological parameters of male Wistar rat. Environ. Sci. Pollut. Res. Int. 31, 4384–4399.
He, Q., et al., 2016. Induction of Poly(ADP-ribose) polymerase in mouse bone marrow stromal cells exposed to 900 MHz radiofrequency fields: preliminary observations. BioMed Res. Int. 2016, 4918691.
He, Q., et al., 2017. Adaptive response in mouse bone marrow stromal cells exposed to 900MHz radiofrequency fields: impact of poly (ADP-ribose) polymerase (PARP). Mutat. Res. 820, 19–25.
Hong, M.N., et al., 2012. Effects of 837 and 1950 MHz radiofrequency radiation exposure alone or combined on oxidative stress in MCF10A cells. Bioelectromagnetics 33, 604–611.
ICNIRP, 2020. ICNIRP guidelines for limiting exposures to electromagnetic fields (100 kHz - 300 GHz). Health Phys. 118, 483–524.

ICNIRP, 2025. Gaps in knowledge relevant to the "ICNIRP guidelines for limiting exposure to time-varying electric, magnetic and electromagnetic fields (100 kHz to 300 GHz). Health Phys. 128, 190–202.
Jalilian, H., et al., 2019. Public exposure to radiofrequency electromagnetic fields in everyday microenvironments: an updated systematic review for Europe. Environ. Res. 176, 108517.
Ji, Y., et al., 2016. Adaptive response in mouse bone-marrow stromal cells exposed to 900-MHz radiofrequency fields: Gamma-radiation-induced DNA strand breaks and repair. J Toxicol Environ Health A 79, 419–426.
Jin, Y.B., et al., 2013. Effects of simultaneous combined exposure to CDMA and WCDMA electromagnetic fields on serum hormone levels in rats. J. Radiat. Res. 54, 430–437.
Jin, Y.B., et al., 2011. One-year, simultaneous combined exposure of CDMA and WCDMA radiofrequency electromagnetic fields to rats. Int. J. Radiat. Biol. 87, 416–423.
Jin, Y.B., et al., 2012. Effects of simultaneous combined exposure to CDMA and WCDMA electromagnetic field on immune functions in rats. Int. J. Radiat. Biol. 88, 814–821.
Kang, K.A., et al., 2014. Effects of combined radiofrequency radiation exposure on levels of reactive oxygen species in neuronal cells. J. Radiat. Res. 55, 265–276.
Kim, H.N., et al., 2012. Analysis of the cellular stress response in MCF10A cells exposed to combined radio frequency radiation. J. Radiat. Res. 53, 176–183.
Kim, H.Y., et al., 2024. Effects of 4G long-term evolution electromagnetic fields on thyroid hormone dysfunction and behavioral changes in adolescent Male mice. Int. J. Mol. Sci. 25.
Kostoff, R.N., Lau, C.G.Y., 2013. Combined biological and health effects of electromagnetic fields and other agents in the published literature. Technol. Forecast. Soc. Change 80, 1331–1349.
LeBel, C.P., et al., 1990. Organometal-induced increases in oxygen reactive species: the potential of 2',7'-dichlorofluorescin diacetate as an index of neurotoxic damage. Toxicol. Appl. Pharmacol. 104, 17–24.
Lee, H.J., et al., 2012. The effects of simultaneous combined exposure to CDMA and WCDMA electromagnetic fields on rat testicular function. Bioelectromagnetics 33, 356–364.
Lee, H.J., et al., 2011a. Lymphoma development of simultaneously combined exposure to two radiofrequency signals in AKR/J mice. Bioelectromagnetics 32, 485–492.
Lee, H.J., et al., 2009. Lack of teratogenicity after combined exposure of pregnant mice to CDMA and WCDMA radiofrequency electromagnetic fields. Radiat. Res. 172, 648–652.
Lee, J.S., et al., 2016. Effects of combined radiofrequency field exposure on amyloid-beta-induced cytotoxicity in HT22 mouse hippocampal neurones. J. Radiat. Res. 57, 620–626.
Lee, K.Y., et al., 2011b. Effects of combined radiofrequency radiation exposure on the cell cycle and its regulatory proteins. Bioelectromagnetics 32, 169–178.
Liu, J., et al., 2024. Assessment of EMF exposure induced by wireless cellular phones in various usage scenarios in France. IEEE Access 13, 123743–123755.
Loor, G., et al., 2010. Menadione triggers cell death through ROS-dependent mechanisms involving PARP activation without requiring apoptosis. Free Radic. Biol. Med. 49, 1925–1936.
López-Furelos, A., et al., 2012. An experimental multi-frequency system for studying dosimetry and acute effects on cell and nuclear morphology in rat tissues. Prog. Electromagn. Res. 129, 541–558.
Mattsson, M.O., et al., 2018. Editorial: effects of combined EMF exposures and Co-exposures. Front. Public Health 6, 230.
Miclaus, S., et al., 2023. An exposimetric electromagnetic comparison of Mobile phone emissions: 5G versus 4G signals analyses by means of statistics and convolutional neural networks classification. Technologies 11, 113.
Mortazavi, S.M.J., et al., 2017. Adaptive response induced by pre-exposure to 915 MHz radiofrequency: a possible role for antioxidant enzyme activity. J Biomed Phys Eng 7, 137–142.
Oztopcu-Vatan, P., et al., 2015. Cytotoxic and apoptotic effects of menadione on rat hepatocellular carcinoma cells. Cytotechnology 67, 1003–1009.
Paffi, A., et al., 2010. Considerations for developing an RF exposure system: a review for in vitro biological experiments. IEEE Trans. Microw. Theor. Tech. 58, 2702–2714.
Romeo, S., et al., 2013. A waveguide applicator for in vitro exposures to single or multiple ICT frequencies. IEEE Trans. Microw. Theor. Tech. 61, 1994–2004.
Romeo, S., et al., 2020. Effects of radiofrequency exposure and Co-Exposure on human lymphocytes: the influence of signal modulation and bandwidth. Ieee Journal of Electromagnetics Rf and Microwaves in Medicine and Biology 4, 17–23.
Sa, D.J., et al., 2009. Apoptosis induction by menadione in human promyelocytic leukemia HL-60 cells. Toxicol. Res. 25, 113–118.
Sannino, A., et al., 2025. Exposure to 26.5 GHz, 5G modulated and unmodulated signal, does not affect key cellular endpoints of human neuroblastoma cells. Sci. Rep. 15, 20614.
Sannino, A., et al., 2024a. Protective effect of radiofrequency exposure against menadione-induced oxidative DNA damage in human neuroblastoma cells: the role of exposure duration and investigation on key molecular targets. Bioelectromagnetics 45, 365–374.
Sannino, A., et al., 2024b. The effect of exposure to radiofrequency LTE signal and coexposure to mitomycin-C in Chinese hamster lung fibroblast V79 cells. Bioelectromagnetics 45, 97–109.
Sannino, A., et al., 2009. Induction of adaptive response in human blood lymphocytes exposed to radiofrequency radiation. Radiat. Res. 171, 735–742.
Sannino, A., et al., 2022. Inhibition of autophagy negates radiofrequency-induced adaptive response in SH-SY5Y neuroblastoma cells. Int. J. Mol. Sci. 23.
Sannino, A., et al., 2019. Treatment with 3-Aminobenzamide negates the radiofrequency-induced adaptive response in two cell models. Int. J. Environ. Res. Publ. Health 16.
Sannino, A., et al., 2014. Adaptive response in human blood lymphocytes exposed to non-ionizing radiofrequency fields: resistance to ionizing radiation-induced damage. J. Radiat. Res. 55, 210–217.
Sannino, A., et al., 2011. Induction of adaptive response in human blood lymphocytes exposed to 900 MHz radiofrequency fields: influence of cell cycle. Int. J. Radiat. Biol. 87, 993–999.
SCENIHR, 2015. Potential Health Effects of Exposure to Electromagnetic Fields (EMF. European Commission, Luxembourg.
Schilling, L.M., et al., 2021. Impact of small-cell deployment on combined uplink and downlink RF exposure compared to the status quo in Mobile networks. In: 51st European Microwave Conference (Eumc). IEEE Xplore, London, UK, pp. 618–621.
Shirai, T., et al., 2017. No adverse effects detected for simultaneous whole-body exposure to multiple-frequency radiofrequency electromagnetic fields for rats in the intrauterine and pre- and post-weaning periods. J. Radiat. Res. 58, 48–58.
Simko, M., et al., 2016. Quality matters: systematic analysis of endpoints related to "Cellular Life" in vitro data of radiofrequency electromagnetic field exposure. Int. J. Environ. Res. Publ. Health 13.
Simko, M., et al., 2025. Exposure to radiofrequency electromagnetic fields and IARC carcinogen assessment: risk of bias preliminary literature assessment for 10 key characteristics of human carcinogens. Mutat. Res., Rev. Mutat. Res. 796, 108545.
SSM, S.R.S.A.-., 2024. Recent Research on Electromagnetic Felds and Health Risk, Nineteenth Report from Ssm's Scientifc Council on Electromagnetic Fields.
Veludo, A.F., et al., 2025. Exploring RF-EMF levels in Swiss microenvironments: an evaluation of environmental and auto-induced downlink and uplink exposure in the era of 5G. Environ. Res. 266, 120550.
Verschaeve, L., 2012. Evaluations of international expert group reports on the biological effects of radiofrequency fields. In: Eksim, A. (Ed.), Wireless Communication Networks - Recent Advances. Intech, Rijeka, Croatia, pp. 523–546.
Zeni, O., et al., 2021. Evidence of bystander effect induced by radiofrequency radiation in a human neuroblastoma cell line. Environ. Res. 196, 110935.
Zeni, O., et al., 2012. Induction of an adaptive response in human blood lymphocytes exposed to radiofrequency fields: influence of the universal mobile telecommunication system (UMTS) signal and the specific absorption rate. Mutat. Res. 747, 29–35.
Zeni, O., Scarfì, M.R., 2012. Experimental requirements for in vitro studies aimed to evaluate the biological effects of radiofrequency radiation. In: Costanzo, S. (Ed.), Microwave Materials Characterization. InTech, Rijeka, Croatia.
Zong, C., et al., 2015. Adaptive response in mice exposed to 900 MHZ radiofrequency fields: bleomycin-induced DNA and oxidative damage/repair. Int. J. Radiat. Biol. 91, 270–276.